Characterization of zeolitic imidazole framework (ZIF-8) catalyst for potential biodiesel production from waste cooking oil (WCO)

Xin Hui Chai[1], *Law Yong* Ng[1,2*], *Ching Yin* Ng[3], *Jia Huey Sim*[1,2], *Ying Pei* Lim[4], and *Josephine Ying Chyi* Liew[5,6]

1Department of Chemical Engineering, Lee Kong Chian Faculty and Science (LKC FES), University Tunku Abdul Rahman, Jalan Sungai Long, Bandar Sungai Long, 43000 Kajang, Selangor, Malaysia
2Centre of Advanced and Sustainable Materials Research (CASMR), Universiti Tunku Abdul Rahman, Jalan Sungai Long, Bandar Sungai Long, Kajang 43000, Selangor Malaysia
3Department of Chemical Engineering, Faculty of Engineering, Technology and Built Environment, UCSI University (Kuala Lumpur Campus), No. 1, Jalan Menara Gading, UCSI Heights (Taman Connaught), 56000 Cheras, Kuala Lumpur, Malaysia
4School of Chemical Engineering, Collage of Engineering, Universiti Teknologi MARA, 40450 Shah Alam, Selangor, Malaysia
5Department of Physics, Faculty of Science, Universiti Putra Malaysia, 43400, UPM Serdang, Selangor, Malaysia
6Nanomaterials Synthesis and Characterization Laboratory, Institute of Nanoscience and Nanotechnology, Universiti Putra Malaysia, 43400, UPM Serdang, Selangor, Malaysia

Abstract. Heteropoly acids (HPAs) catalysts prove effective in waste cooking oil biodiesel production, considering their high density of Brønsted acidic sites, exhibit significant resilience to elevated levels of free fatty acid (FFA) and moisture content. However, the separation of HPA catalysts after biodiesel production is challenging due to their homogeneous catalytic nature. This study aims to develop magnetic vanadium-substituted HPA-based ZIF-8 composites to create a catalyst for biodiesel production from WCO that is more efficient and easier to separate. In this work, a range of analytical methods was utilized to characterize the catalyst, such as Fourier-transform infrared spectroscopy (FTIR), scanning electron microscopy coupled with energy dispersive X-ray spectroscopy (SEM-EDX), high-resolution transmission electron microscopy (HRTEM), and a vibrating sample magnetometer (VSM). The successful incorporation of HPA acid into the magnetite ZIF-8 nanocomposite was indicated by prominent bands in the FTIR analysis, and this formation was further validated by EDX analysis. The VSM results also revealed that the nanocomposite has good magnetic responsiveness, facilitating catalyst separation and recycling. The magnetic ZIF-8 composites functionalized with $H_6PV_3MoW_8O_{40}$ demonstrated significant potential for sustainable biodiesel production from WCO.

*Corresponding author: lyng@utar.edu.my

1 Introduction

The use of non-renewable energy poses significant ecological challenges, exacerbated by industrial advancements and technological evolution. Fossil fuels like coal, crude oil, and natural gas are widely used in various industries and transportation, contributing to global warming, environmental pollution, and ozone layer depletion. In 2023, CO_2 emissions reached 37.4 billion tonnes, further increasing atmospheric CO_2 levels and global temperatures [1, 2]. This has prompted the global research community to explore alternative energy sources, such as biodiesel, known for its lubricating and oxidation properties [3].

Edible oils (e.g., sunflower, soybean, olive) have been used as renewable feedstocks for biodiesel production, raising concerns about competition with food supplies. To address this, waste cooking oil (WCO) offers a promising alternative. However, the choice of catalyst is crucial; base catalysts can lead to soap formation due to reactions with WCO's free fatty acids (FFAs) and water content [4, 5]. Acidic catalysts, on the other hand, are more effective for biodiesel production, as they are not affected by FFAs and can catalyze both esterification and transesterification reactions [6].

The study aims to develop heteropoly acids (HPAs) that can potentially be used for biodiesel production. Specifically, the objectives include producing HPAs with high catalytic efficiency and stability for biodiesel production from WCO. Heterogeneous catalysts, especially HPAs, are gaining attention over homogeneous catalysts due to easier separation and recovery. HPAs are highly effective for biodiesel production due to their strong acidity and tolerance for high FFA and moisture content [7]. However, their low surface area and solubility in polar media pose challenges, which can be mitigated by immobilizing HPAs onto porous supports [8]. The modified HPA, $H_6PV_3MoW_8O_{40}$, shows promise for biodiesel production due to its high activity and insolubility in methanol [9].

Metal-organic frameworks (MOFs), with Zeolitic Imidazole Framework (ZIF-8) being a prominent example, are gaining recognition as highly efficient catalysts. This is attributed to their exceptional surface area, remarkable thermal stability, and the presence of diverse, tunable catalytic sites [10, 11, 12]. ZIF-8 exhibits a surface area ranging from 1400 to 3000 m^2/g and stability up to 420°C, can be magnetized for easy separation from the reaction medium [13]. The impregnation of $H_6PV_3MoW_8O_{40}$ onto magnetized ZIF-8 is expected to yield excellent catalytic performance for economical biodiesel production from low-grade acidic oils.

2 Materials and methods

2.1 Materials

2-Methylimidazole ($C_4H_6N_2$ ≥ 98%), hydrochloric acid (HCl ≥ 98%), sulphuric acid (H_2SO_4 ≥ 98%), sodium tungstate dihydrate ($Na_2WO_4{\cdot}2H_2O$ ≥ 99%), sodium metavanadate ($Na_2MoO_4{\cdot}2H_2O$ ≥ 99%), sodium dihydrogen phosphate (NaH_2PO_4 ≥ 99%), and sodium molybdate dihydrate ($Na_2VO_3{\cdot}2H_2O$ ≥ 99%) were obtained from Macklin (Shanghai, China) and Systerm (Selangor, Malaysia).

2.2 Preparation of Fe_3O_4 magnetic nanoparticles

Primarily, the synthesis of iron (III) oxide (Fe_3O_4) nanoparticles was accomplished through the co-precipitation method as denoted in the available literature [1]. 4.44g of iron (III) chloride, hexahydrate ($FeCl_3{\cdot}6H_2O$) and 4.56g of iron (II) sulphate ($FeSO_4{\cdot}7H_2O$) were dissolved in 80mL of 0.1M HCl solution. Subsequently, the mixture underwent heating to

80℃ through a heating plate while undergoing magnetic stirring while a 60mL volume of 3M ammonia was gradually introduced into the solution drop by drop. The mixture was allowed to heat and stir continuously for 3 hours. The Fe_3O_4 nanoparticles were filtered and washed with an equal molar ratio of ethanol and water solution. Finally, Fe_3O_4 nanoparticles were obtained by drying the black powder in a vacuum oven at 60℃ for 12 hours.

2.3 Preparation of magnetite ZIF-8 nanoparticles

The one-pot synthesis was adopted to prepare the magnetite ZIF-8 nanoparticles [1]. 0.1g of the afore-prepared Fe_3O_4, 0.238g of hexahydrate zinc nitrate ($Zn(NO_3)_2{\cdot}6H_2O$), and 0.657g of 2-MIM were dissolved in 30mL of ethanol. The mixture was then ultrasonicated for 30 minutes at 60℃ whereby a 10μL of 37% HCl was slowly added to the mixture [2]. Following sonication, the mixture was stirred at room temperature for 10 minutes. The obtained powder was then filtered and rinsed using a solution composed of ethanol and water in equal molar proportions. Finally, magnetite ZIF-8 nanoparticles were produced by drying the powder in a vacuum oven at 90℃ for 12 hours.

2.4 Preparation of $H_6PV_3MoW_8O_{40}$ acid

A homogeneous mixing of 70mL of $Na_2WO_4{\cdot}2H_2O$ (0.08 mol), 20mL of $Na_2VO_3{\cdot}2H_2O$ (0.03 mol), and 20mL of NaH_2PO_4 (0.01 mol) was achieved through magnetic stirring. A 50% v/v sulphuric acid solution was incorporated dropwise to the mixture until the pH reached 2.6. Then 10mL of $Na_2MoO_4{\cdot}2H_2O$ (0.01 mol) was blended into the mixture and the resulting mixture was stirred at 75℃ for 3 hours. After cooling to ambient temperature, the mixture was transferred to a separatory funnel and vigorously combined with diethyl ether. The denser phase was then separated, and any remaining diethyl ether was evaporated by heating the solution to 40°C.

2.5 Preparation of $H_6PV_3MoW_8O_{40}$ functionalized magnetite ZIF-8

The functionalized magnetite ZIF-8 was synthesized by adding the prepared magnetite ZIF-8 nanoparticles to the $H_6PV_3MoW_8O_{40}$ acid solution [3]. In detail, 1.5g of magnetite ZIF-8 support was dispersed in 150mL of $H_6PV_3MoW_8O_{40}$ acid solution. The resulting solution was ultrasonicated at 60℃ for 1 hour and then vigorously stirred for 24 hours with an overhead stirrer. The powder was separated by filtration and rinsed with distilled water. Subsequently, it was dried in a vacuum oven at 60°C for 12 hours, resulting in the formation of $H_6PV_3MoW_8O_{40}$ functionalized magnetite ZIF-8.

2.6 Characterization of the ZIF-8 nanocomposite

The synthesized catalysts were then characterized using various analytical techniques. Fourier transform infrared (FTIR) spectra were obtained using the Thermo Nicolet system at frequencies ranging from 400 to 4000cm^{-1} with a spectral resolution of 4cm^{-1}. The catalyst morphology was observed using the scanning electron microscope (SEM, LEO 1450 VP) equipped with an energy-dispersive X-ray, utilising a 15kV accelerating voltage. Transmission electron microscopy (TEM) micrographs were examined using a JSM-6390LV TEM running at 200kV accelerating voltage. Also, the vibrating sample magnetometer (VSM, LakeShore model 7304) was used to evaluate the magnetic characteristics of the prepared catalysts.

3 Results and discussion

3.1 Catalyst characterization

3.1.1 Chemical properties

Figure 1 depicts the FTIR spectra for the sample of ZIF-8, Fe_3O_4/ZIF-8, and $H_6PV_3MoW_8O_{40}/Fe_3O_4$/ZIF-8. According to Figure 1 (a), several noticeable bands could be observed at the wavenumber of 1584 cm^{-1}, 1300-1460 cm^{-1}, 1146 cm^{-1}, 994 cm^{-1}, 759 cm^{-1}, 693 cm^{-1} and 420 cm^{-1} by which these FTIR bands corresponded to the adsorption vibration modes of the imidazole groups in ZIF-8 MOF and had been reported by Zhang et al., (2018)[4]. In this instance, the 3147 cm^{-1} and 1584 cm^{-1} peaks may be linked to aromatic C-H asymmetric stretching and C=N stretch vibration. Also, there were signs for the complete ring stretching at wavenumber ranging 1300-1460 cm^{-1}. The band at 1146 cm^{-1} could be attributed to the aromatic C-N stretching mode, whereas the peaks at 994 cm^{-1} and 694 cm^{-1} may correspond to the C-N bending vibration and the C-H bending mode, respectively. The ring out-of-plane bending vibration of the HmIm was the result of the band at 693 cm^{-1} and the band at 420 cm^{-1} is ascribed to the Zn-N stretch. As observed in Figure 1 (b), the bands at 3147 cm^{-1} and 1636 cm^{-1} in the FTIR spectrum of Fe_3O_4 might be attributed to the hydroxyl groups of Fe_3O_4 or generated by the adsorption of water, which resembles previously published information [1]. The 600-1500 cm^{-1} peaks can be attributed to the stretching or bending of the entire ring contributed by ZIF-8 MOF, evaluating the occurrences of Fe_3O_4 and ZIF-8 in the composite substrate produced [1], [3]. Lastly, the stretching vibrations of the primary Keggin-type POM structure ν_{as}(P-O_a), ν_{as}(M-O_d), ν_{as}(M-O_b-M), and ν_{as}(M-O_c-M) are responsible for the prominent bands detected in the FTIR spectra of the $H_6PV_3MoW_8O_{40}/Fe_3O_4$/ZIF-8 at 1075 cm^{-1}, 994 cm^{-1}, 884 cm^{-1}, and 757 cm^{-1} [3]. In this case, the distinctive IR bands associated with the ZIF-8 and Fe_3O_4/ZIF-8 were retained as illustrated in Figure 1(c), implying that the magnetic ZIF-8 support was loaded with HPAs.

To further verify the successful formation of $H_6PV_3MoW_8O_{40}/Fe_3O_4$/ZIF-8, the elemental analysis is conducted using the EDX as illustrated in Figure 2. In this occurrence, the elements Fe, Zn, C, O, and W that are visible in the original structure of $H_6PV_3MoW_8O_{40}/Fe_3O_4$/ZIF-8 clearly show that ZIF-8 and $H_6PV_3MoW_8O_{40}$ successfully formed alongside Fe_3O_4 [1], [5].

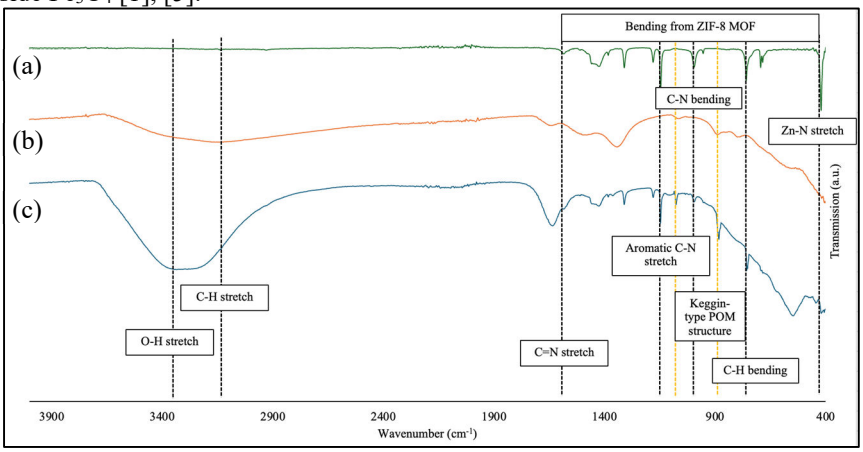

Fig 1. FTIR spectra of ZIF-8 (a), Fe_3O_4/ZIF-8 (b), and $H_6PV_3MoW_8O_{40}/Fe_3O_4$/ZIF-8 (c) sample.

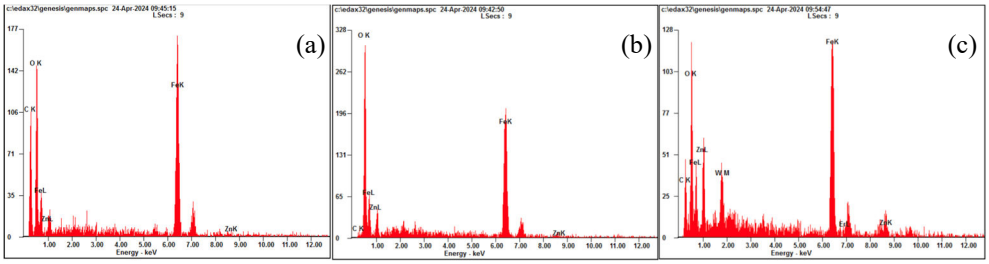

Fig 2. EDX analysis of ZIF-8 (a), Fe_3O_4/ZIF-8 (b), and $H_6PV_3MoW_8O_{40}$/Fe_3O_4/ZIF-8 (c) sample.

3.1.2 Morphological study

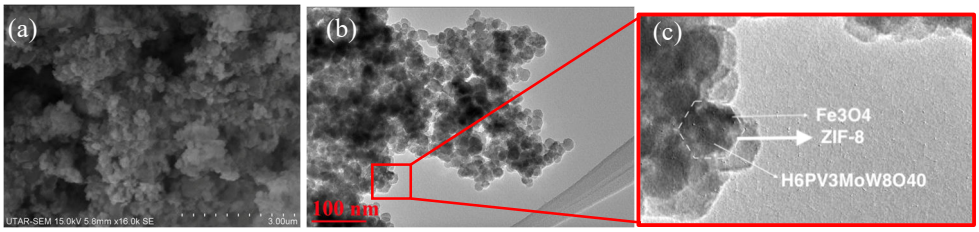

Fig 3. (a) SEM image (left), (b) and (c) HRTEM images (right) of $H_6PV_3MoW_8O_{40}$/Fe_3O_4/ZIF-8.

The morphology of the $H_6PV_3MoW_8O_{40}$/Fe_3O_4/ZIF-8 was examined using SEM and HRTEM as shown in Figure 3. From the SEM image, a spherical morphology with a smoother surface was observed in the synthesized solid catalyst [3]. The synthesis of $H_6PV_3MoW_8O_{40}$/Fe_3O_4/ZIF-8 nanocomposite catalyst with an average size of around 15.52 nm was confirmed by observing the $H_6PV_3MoW_8O_{40}$ nanoparticles dispersed randomly in the hexagonal magnetic ZIF-8 [1], [3]. Such dispersion may ease the access of reactants to the acidic sites, making the reaction simple to conduct. The solid catalyst's structure is particularly noteworthy due to the robust interactions between the imidazole groups in ZIF-8 and the Keggin structure of HPAs. These interactions effectively prevent HPAs from leaching from the magnetic support, thereby increasing the catalyst's reusability.

3.1.3 Magnetic behaviour

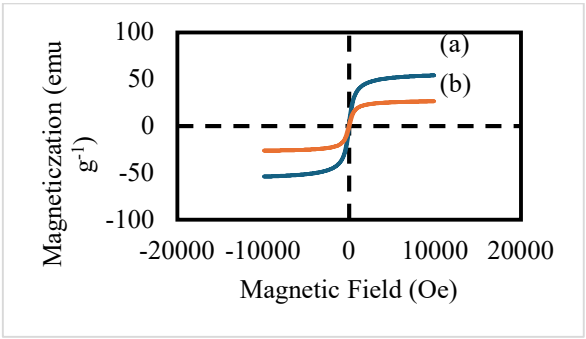

Fig 4. Magnetic hysteresis Fe_3O_4/ZIF-8 (a), and $H_6PV_3MoW_8O_{40}$/Fe_3O_4/ZIF-8 (b) sample.

Figure 4 displays the magnetization hysteresis curves for the Fe_3O_4/ZIF-8 and $H_6PV_3MoW_8O_{40}$/Fe_3O_4/ZIF-8 samples by which the magnetic behavior of these catalysts was accessed using VSM. The isothermal magnetization curves for the two samples exhibited an

S-shaped pattern, rapidly increasing magnetization upon applying a magnetic field at room temperature. As a result of incorporating non-magnetic ZIF-8 MOFs, the saturation magnetization of the Fe_3O_4 magnetite was reduced to 54.11 emu/g, which was lower than 86.7 emu/g for the Fe_3O_4 magnetite as previously reported [3]. The generated $H_6PV_3MoW_8O_{40}/Fe_3O_4$/ZIF-8 catalyst's saturation magnetization was further reduced to 26.47 emu/g following the loading of the HPAs. However, owing to the robust magnetic responsiveness of the solid catalyst to an external permanent magnet, its facile recycling through the application of an external magnetic field enables the performance of magnetic separation and interconnectivity.

4 Conclusion

The $H_6PV_3MoW_8O_{40}/Fe_3O_4$/ZIF-8 catalyst was eventually prepared by incorporating Fe_3O_4 nanoparticles into ZIF-8 MOF followed by loading $H_6PV_3MoW_8O_{40}$ on the magnetic Fe_3O_4/ZIF-8 composites. The $H_6PV_3MoW_8O_{40}/Fe_3O_4$/ZIF-8 catalyst was successfully synthesized, as shown by the FTIR and EDX analyses. The identification of vibrational absorption modes associated with the imidazole groups of the ZIF-8 MOF, the Fe-O stretching vibrations in Fe_3O_4, and the principal Keggin-type POM structure verified the synthesized $H_6PV_3MoW_8O_{40}/Fe_3O_4$/ZIF-8 catalyst. Furthermore, the EDX analysis revealed the presence of Fe, Zn, C, O, and W elements in the catalysts. Also, the strong interactions between the ZIF-8's imidazole groups and the Keggin structure of the HPAs have been observed using the SEM and HRTEM. These interactions effectively prevent the HPAs from leaching from the magnetic support, increasing the catalyst's reusability. The average particle size of 15.52nm could enhance the accessibility of the reactants to the catalyst's active sites, potentially leading to a high reaction rate. Lastly, the synthesized catalyst can be readily recycled by an external magnetic field as the solid catalyst showed a favourable response to an external permanent magnet, displaying good magnetic responsiveness during the VSM analysis.

The authors would like to acknowledge the financial support received from the Fundamental Research Grant Scheme (FRGS) under grant number (FRGS/1/2023/STG05/UPM/02/3) from the Ministry of Higher Education Malaysia and research grant (UPM-JORDAN/2022/9300486) from Universiti Putra Malaysia.

References

1. International Energy Agency, I., CO 2 Emissions in 2023. (2023)
2. O.A. Marzouk, Expectations for the Role of Hydrogen and Its Derivatives in Different Sectors through Analysis of the Four Energy Scenarios: IEA-STEPS, IEA-NZE, IRENA-PES, and IRENA-1.5℃. Energies. **17**, (2024). https://doi.org/10.3390/en17030646
3. S. Firoz, A review: Advantages and Disadvantages of Biodiesel. Int. Res. J. Eng. Technol. **4**, 530-535 (2008).
4. W. Xie, C. Gao, J. Li, Sustainable biodiesel production from low-quantity oils utilizing H6PV3MoW8O40 supported on magnetic Fe3O4/ZIF-8 composites. Renew. Energy. **168**, 927–937 (2021). https://doi.org/10.1016/j.renene.2020.12.129
5. B. Cheirsilp, S. Srinuanpan, Y.I. Mandik, Efficient Harvesting of Microalgal biomass and Direct Conversion of Microalgal Lipids into Biodiesel. Microalgae Cultiv. Biofuels Prod. **3**, 83–96 (2020). https://doi.org/10.1016/B978-0-12-817536-1.00006-0

6. V. Mandari, Santhosh, K. Devarai, Biodiesel Production Using Homogeneous, Heterogeneous, and Enzyme Catalysts via Transesterification and Esterification Reactions: a Critical Review. Bioenergy Res. https://doi.org/10.1007/s12155-021-10333-w
7. F. Esmi, V.B. Borugadda, A.K. Dalai, Heteropoly acids as supported solid acid catalysts for sustainable biodiesel production using vegetable oils: A review. Catal. Today. **404**, 19–34 (2022). https://doi.org/10.1016/j.cattod.2022.01.019
8. W. Xie, X. Wang, L. Guo, Boosting biodiesel production from acidic oils using tin-doped tungstophosphoric acid embedded on ZIF-8 with Brönsted-Lewis acid sites as a reusable catalyst. Biomass Bioenergy. **181**, (2024). https://doi.org/10.1016/j.biombioe.2024.107064
9. L. Guo, W. Xie, C. Gao, Heterogeneous H6PV3MoW8O40/AC-Ag catalyst for biodiesel production: Preparation, characterization and catalytic performance. Fuel. **316**, (2022). https://doi.org/10.1016/j.fuel.2022.123352
10. M.S. Alhumaimess, Metal–organic frameworks and their catalytic applications. J. Saudi Chem. Soc. **24**, 461-473 (2020). https://doi.org/10.1016/j.jscs.2020.04.002
11. J.V.L. Ruatpuia, G. Halder, S. Mohan, B. Gurunathan, H. Li, F. Chai, S. Basumatary, S. Lalthazuala Rokhum, Microwave-assisted biodiesel production using ZIF-8 MOF-derived nanocatalyst: A process optimization, kinetics, thermodynamics and life cycle cost analysis. Energy Convers Manag. **292**, (2023). https://doi.org/10.1016/j.enconman.2023.117418
12. Y.R. Lee, X.H. Do, S.S. Hwang, K.Y. Baek, Dual-functionalized ZIF-8 as an efficient acid-base bifunctional catalyst for the one-pot tandem reaction. Catal Today. **359**, 124–132 (2021). https://doi.org/10.1016/J.CATTOD.2019.06.076
13. M.O. Abdelmigeed, E.G. Al-Sakkari, M.S. Hefney, F.M. Ismail, A. Abdelghany, T.S. Ahmed, I.M. Ismail, Magnetized ZIF-8 impregnated with sodium hydroxide as a heterogeneous catalyst for high-quality biodiesel production. Renew. Energy. *165*, pp.405-419.
14. A. Moatamed Sabzevar, M. Ghahramaninezhad, M. Niknam Shahrak, Enhanced biodiesel production from oleic acid using TiO2-decorated magnetic ZIF-8 nanocomposite catalyst and its utilization for used frying oil conversion to valuable product. Fuel. **288**, (2021). https://doi.org/10.1016/j.fuel.2020.119586
15. C. Yim, H. Lee, S. Lee, S. Jeon, One-step immobilization of antibodies on ZIF-8/Fe3O4 hybrid nanoparticles for the immunoassay of Staphylococcus aureus. RSC Adv. **7**, 1418–1422 (2017). https://doi.org/10.1039/C6RA25527B
16. Y. Zhang, Y. Jia, L. Hou, Synthesis of zeolitic imidazolate framework-8 on polyester fiber for PM2.5 removal. RSC Adv. **8**, 31471–31477 (2018). https://doi.org/10.1039/c8ra06414h
17. A. Moussa, A. Rahmati, A. One-Pot Synthesis of Benzo[4,5]imidazo[1,2-a]pyrimidin-2-ones Using a Hybrid Catalyst Supported on Magnetic Nanoparticles in Green Solvents. Chem. Open. **10**, 764–774 (2021). https://doi.org/10.1002/open.202100063